

# THE INTERNATIONAL JOURNAL OF SCIENCE & TECHNOLEDGE

## Spectral, Optical, Mechanical Properties of Lithium Doped Nonlinear Optical Crystal L-Lysine Monohydrochloride

**S. Chennakrishnan**

Department of Physics, Idhaya Arts & Science College for women, Tiruvannamalai, India

**D. Sivavishnu**

P. G. and Research Department of Physics, Government Arts College, Tiruvannamalai, India

**S.M. Ravikumar**

P. G. and Research Department of Physics, Government Arts College, Tiruvannamalai, India

### **Abstract:**

The cell and structural parameters of grown crystal were determined by single crystal x-ray diffraction analysis. The characteristic functional groups in the compound were identified from Fourier transform infrared spectroscopy. The transmission spectrum of this crystal show that the lower cut-off wavelength lies at 234 nm. The optical constant of the grown crystal like band gap, refractive index, reflectance, extinction coefficient and electrical susceptibility were also determined from UV-Vis-NIR spectrum. The powder second harmonic generation efficiency of the grown crystal measured by Kurtz technique is 0.55 times that of potassium dehydrogenate phosphate (KDP). Vicker's microhardness test showed that the hardness value increases with increasing the applied load upto 100 g.

### **1. Introduction**

Non-linear optical (NLO) crystals appear to be very attractive for applications in image processing and optical communication. Materials with large second order optical nonlinearities, short transparency cutoff wavelength and stable physical and thermal performance are needed in order to realize many of these applications [1-4]. Though organic NLO crystals have high non-linearity, fast responses and tailer made flexibility [5,6]. Their applications are limited due to inherent poor chemical stability, poor phase matching and red shift of the cut off wavelength caused by large organic  $\pi$ -conjugated system [7].

It is difficult to grow large optical quality crystal of these materials for device applications [8,9]. The merits are retained and the short comings are overcome when the choice switches to semi-organic complex crystals. Recently a number of semi-organic crystals for NLO applications have been explored due to their non-linearity, high resistance to laser-induced damage, low angular sensitivity and good mechanical hardness [10-14].

Amino acids and their complexes belong to family organic materials that have been considered for photonic applications. L-arginine and L-arginine phosphate, L-alanine, glutamic acid, and  $\gamma$ -glycine evidently showing NLO activity because of an additional COOH group in first and NH<sub>2</sub> in the second carbon [15,16]. In the present work, attempts have been made to improve the physicochemical properties by incorporating metal with L-Lysine monohydro chloride. Hence, the effect of lithium chloride on growth of L-Lysine monohydro chloride crystal has been discussed.

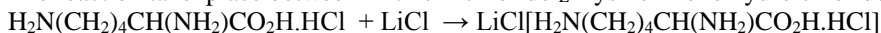
Several researches have reported the growth and other properties of L-Lysine mono hydro chloride [17-22], and to the best of our knowledge this is the first report regarding the spectral, optical, mechanical properties of lithium doped L-lysine monohydrochloride and the results are discussed.

### **2. Experimental Procedure**

#### *2.1. Material Synthesis*

Initially, Lithium L-Lysine monohydrochloride Li[L-LMHCl] was prepared by mixing synthesized by taking lithium chloride (AR grade) and l-lysine monohydrochloride (AR grade) in molar ratio 1:1 using double-distilled water. The solution was stirred well about 4 hours to form homogeneous solution. The homogeneous mixture solution was filtered twice with whatmann filter paper to remove impurities. This supersaturated solution was tightly covered with plastic paper to keep out dust before it was slowly allowed to evaporate at room temperature.

The reaction take place between Lithium chloride L-Lysine mono hydro chloride in water medium as follows.



#### *2.2. Crystal Growth*

Optically transparent and defect free crystals of Li[L-LMHCl] were obtained by the self-nucleation of the saturated solution [PH=3] by slow evaporation. Bulk size crystal of size 10 x 5 x 2 mm<sup>3</sup> was harvested in the period 30-35 days. The grown crystal has colourless, transparent, defect free from impurities and non-hygroscopic nature. The grown crystal of Li [L-LMHCl] is shown in the figure 1.

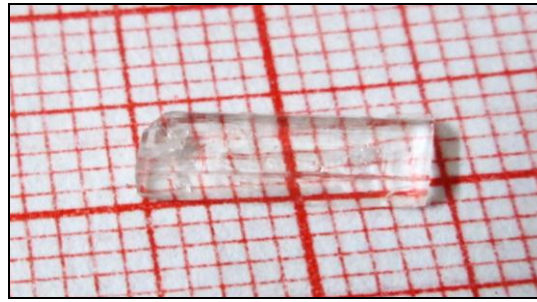


Figure 1: As grown crystal of Li [L-LMHCl]

### 3. Result and Discussion

#### 3.1. Single Crystal XRD Analysis

The title compound was analysed by single crystal XRD method by ENRAF NONIUS CAD4-F single X-ray diffractometer with  $\text{MoK}\alpha$  ( $\lambda=0.717\text{\AA}$ ) radiation. It is observed that the grown crystal crystallizes in monoclinic system with space group  $p2_1$ . The calculated lattice parameter for pure L-LMHCl was found to be  $a=5.91\text{\AA}$ ,  $b=13.39\text{\AA}$ ,  $c=7.54\text{\AA}$  and volume,  $V=596.67\text{\AA}^3$ . For Li[L-LMHCl] crystals, the lattice parameters are  $a=5.88\text{\AA}$ ,  $b=13.35\text{\AA}$ ,  $c=7.53\text{\AA}$  and volume  $V=591.08\text{\AA}^3$ , whereas for doped L-LMHCl crystals,  $a=5.87\text{\AA}$ ,  $b=13.33\text{\AA}$ ,  $c=7.50\text{\AA}$  and volume  $V=586.85\text{\AA}^3$ .

Thus the XRD result conforms the incorporation of metal ions in the crystal lattice of L-LMHCl but do not change the crystal structure though there is a small change in the lattice parameters.

#### 3.2. FTIR Analysis

The FTIR spectroscopy studies are effectively used to identify the functional groups, presents in the grown crystal and to determine the molecular structure. In order to analyse qualitatively the presence of functional groups, freshly crushed powder of Li[L-LMHCl] crystal was subjected to FTIR studies using thermo Nicolect v-200 FTIR spectrometer by KBr pellet method in the range  $500\text{--}4000\text{ cm}^{-1}$ .

Figure 2, shows FTIR spectrum of Li[L-LMHCl] crystal. The absorbed frequencies and their assignment of Li[L-LMHCl] crystals are shown in the table 1. The broad band in the higher energy region around  $3164\text{ cm}^{-1}$  is due to  $\text{NH}_3^+$  asymmetric stretching. The strong but broad peaks observed at  $2931\text{ cm}^{-1}$  due to presence of C-H asymmetric stretching. The C-H stretching and bending is at  $2620$  and  $1352\text{ cm}^{-1}$  respectively. The absorption band at  $2113\text{ cm}^{-1}$  is due to the combination of  $\text{NH}_3^+$  deformation and  $\text{NH}_3^+$  torsion. The peak at  $1617\text{ cm}^{-1}$  is attributed to  $\text{NH}_3^+$  asymmetric deformation. The peak observed at  $1508\text{ cm}^{-1}$  implies  $\text{NH}_3^+$  stretching. The  $\text{COO}^-$  symmetric stretching vibrations are observed at  $1411\text{ cm}^{-1}$ . The peak observed at  $1282\text{ cm}^{-1}$  is due to C-N-stretching. The C-C stretching at  $996$  and  $908\text{ cm}^{-1}$ . The C-C-N symmetric and asymmetric stretching is found at  $861$  and  $1096\text{ cm}^{-1}$ . The band appearing at  $739\text{ cm}^{-1}$  infers the C-O-H stretching of the pure crystals which are all very well agreed with literature. The scissoring and wagging vibrations of  $\text{NH}_3^+$  groups are observed at  $710$  and  $554\text{ cm}^{-1}$ . The absorption peak at  $668\text{ cm}^{-1}$  is due to the C-Cl stretching. The assignments confirm the presence of various functional groups present in the material, tabulated in table 1.

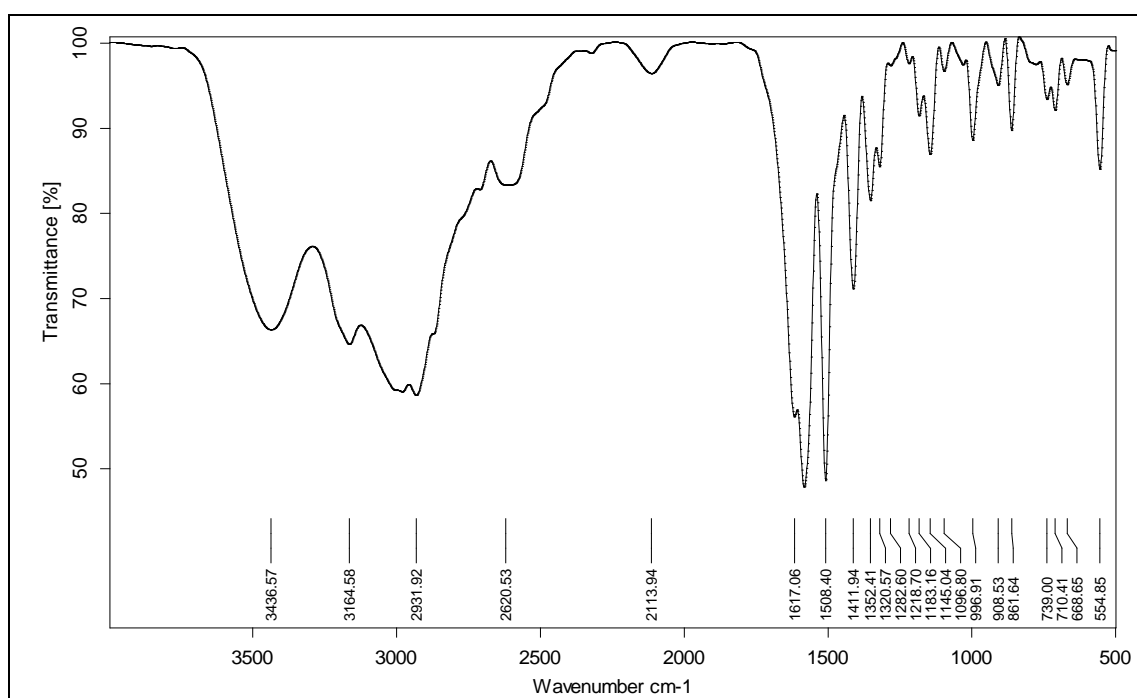


Figure 2: FTIR spectrum of Li [L-LMHCL]

Wavenumbers $\text{cm}^{-1}$	Assignments
3436	O-H bending(for pure L-LMHCL)
3164	$\text{NH}_3^+$ asymmetric stretching
2931	C-H asymmetric stretch
2620	C-H stretching
2113	Combination of $\text{NH}_3^+$ deformation and $\text{NH}_3^+$ torsion
1617	$\text{NH}_3^+$ asymmetric deformation
1508	$\text{NH}_3^+$ stretching
1411	$\text{COO}^-$ symmetric stretching
1352	C-H bending
1282	C-N stretching
1145	$\text{NH}_3^+$ rocking
1096	C-C-N asymmetric stretching
996	C-C stretching
861	C-C-N symmetric stretch, O-H..O out of plane bending
739	C-O-H stretching
668.55	C-Cl stretching

Table 1: Assignment of IR band frequencies ( $\text{cm}^{-1}$ ) observed for grown crystal  $\text{Li}[\text{L-LMHCL}]$

### 3.3. Linear Optical Studies

The UV-visible spectrum of the synthesized compound has been recorded using DOUBLE BEAM UV-Vis spectrophotometer:2202 in the region 0- 600 nm and the spectrum shown in figure.3. Optically polished single crystal of thickness 2mm was used for this study.

The title crystal is active in the entire UV-vis region. The grown crystal was very transparent (99%) and colourless and there is no absorption in the entire visible region. But around 234 nm there is sharp decrease in transmittance, due to absorption leading to excitation in this region.

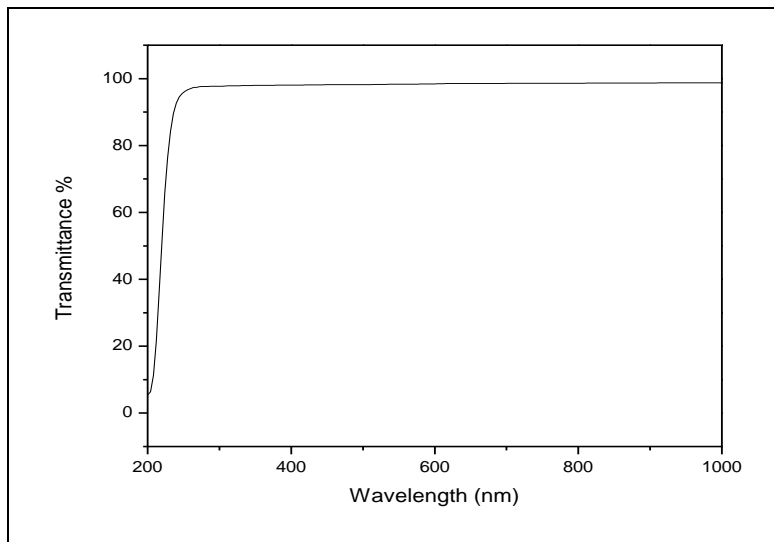


Figure 3: Optical transmittance spectra of  $\text{Li}[\text{L-LMHCL}]$  crystal

### 3.4 Determination of Optical Bandgap and Optical Constants

The measured transmittance (T) using optical transmittance spectrum was used to calculate the absorption coefficient ( $\alpha$ ) using the formula

$$\alpha = \frac{2.3026 \log\left(\frac{1}{T}\right)}{t}$$

Where, T is the transmittance and t is the thickness of the crystal.

Optical band gap ( $E_g$ ) has been evaluated from the transmission spectra and the optical absorption coefficient ( $\alpha$ ) near the absorption edge is given by

$$h\nu = A(h\nu - E_g)^{1/2}$$

Where A is a constant,  $E_g$  the optical bandgap, h the planck’s constant and  $\nu$  the frequency of incident photons. The band gap of  $Li[Li-LMHCL]$  crystal was estimated by plotting  $(\alpha h\nu)^2$  versus  $h\nu$  as shown in the Figure 4. The value of bandgap was found to be 5.7 eV. The wide band gap of the  $Li[Li-LMHCL]$  crystal confirms the large transmittance in the visible region [19] and this crystal can be suitable for the optoelectronic devices like laser diode [20].

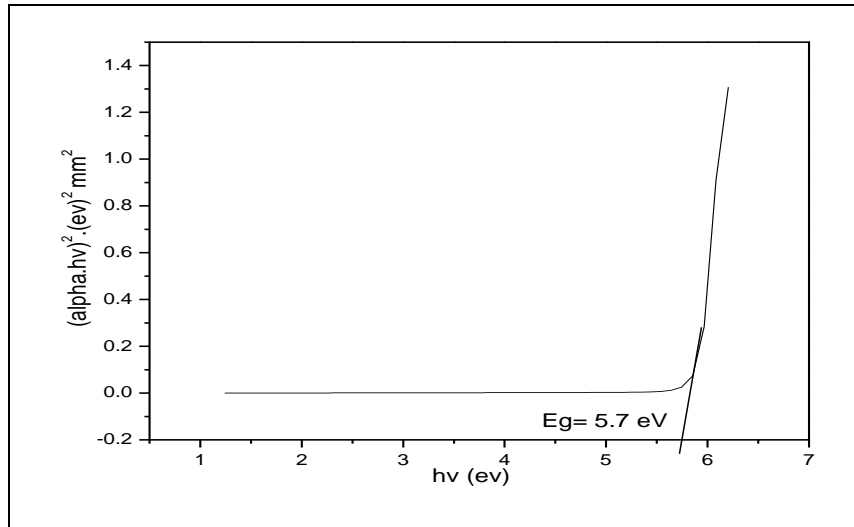


Figure 4: Tauc’s plot of  $Li[Li-LMHCL]$  crystal

Extinction coefficient (K) can be obtained from the following equation

$$K = \frac{\lambda\alpha}{4\pi}$$

The extinction coefficient as a function of absorption coefficient ( $\alpha$ ) is shown in Figure 5. The transmittance (T) is given by [23]

$$T = \frac{(1 - R)^2 \exp(-\alpha t)}{1 - R^2 \exp(-2\alpha t)}$$

The reflectance (R) in terms of the absorption coefficient can be obtained from the above equation. Hence,

$$R = \frac{\exp(-\alpha t) \pm \sqrt{\exp(-\alpha t) T - \exp(-3\alpha t) + \exp(-2\alpha t) T^2}}{\exp(-\alpha t) + \exp(-2\alpha t) T}$$

The refractive index (n) can be determined from reflectance data using the equation.

$$n = \frac{-(R + 1) \pm 2\sqrt{R}}{(R - 1)}$$

The absorption coefficient versus reflectance is shown in the Figure 6. Figure 7 represents the variation of refractive index as a function of wavelength. The refractive index (n) decrease with increase in wavelength indicates that the grown sample absorbs at lower wavelength region. The variation of n and K values with respect to wavelength reveals the interaction of photon with electron. The refractive index ‘n’ is 1.44 at 1000 nm and the refractive index is strongly dependent on wavelength.

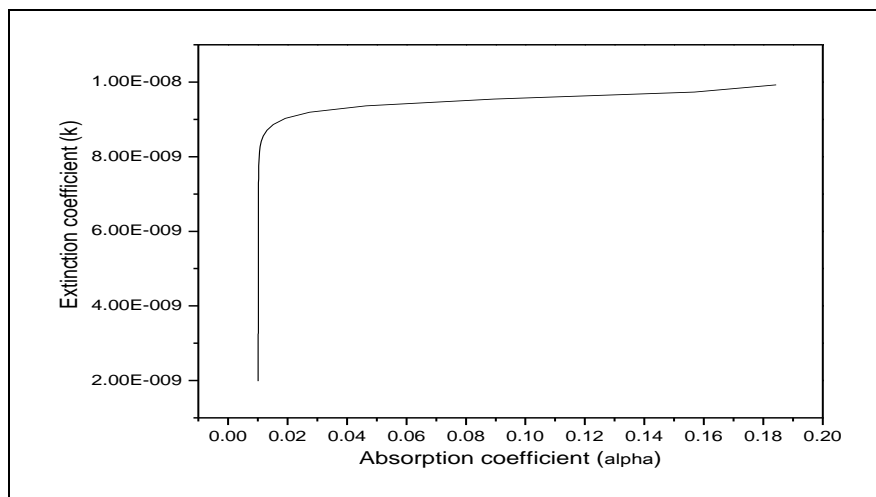


Figure 5: A plot of extinction coefficient versus absorption coefficient of  $Li[Li-LMHCL]$  crystal

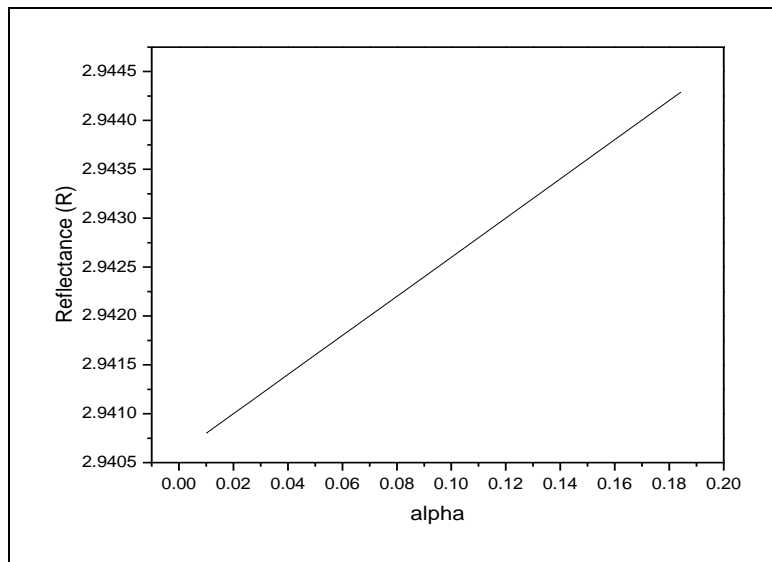


Figure 6: Absorption coefficient Vs reflectance of Li[ L-LMHCL] crystal

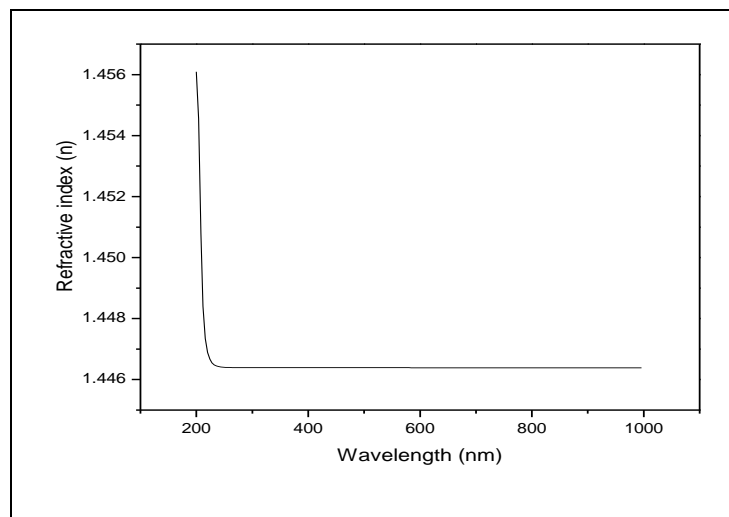


Figure 7: Plot of refractive index versus photon energy for Li[ L-LMHCL] crystal

The electrical susceptibility ( $\chi_c$ ) can be calculated using the following relation,

$$\chi_c = \epsilon_r - 1$$

$$\text{(or)} \quad \chi_c = n^2 - 1 \text{ (i.e., } \epsilon_r = n^2 \text{).}$$

Hence, Susceptibility = 1.07.

Since electrical susceptibility is greater than 1, the material can be easily polarised when the incident light is more intense.

### 3.5. Powder SHG Measurement

The nonlinear optical property of the grown crystal is tested by passing the output of Nd:YAG Quanta ray laser through the crystalline powder sample. A Q-switched, mode locked Nd: YAG laser was used to generate about 6 mJ/pulse at the 1064 nm fundamental radiation. This laser can be operated in two modes. In the single shot mode the laser emits a single 8 ns pulse. In the multi shot mode the laser produces a continuous train of 8 ns pulses at a repetition rate of 10 Hz. In the present study, a single shot mode of 8 ns laser pulse with a spot radius of 1mm was used.

This experimental setup used a mirror and a 50/50 beam splitter (BS) to generate a beam with pulse energies about 6 mJ. The input laser beam was passed through an IR reflector and then directed on the micro crystalline powdered sample packed in a capillary tube of a diameter 0.154 mm. The photodiode detector and oscilloscope assembly measured the light emitted by the sample. Microcrystalline powder of urea or KDP is taken in a similar capillary tube sealed at one end for comparison. The intensity of the second harmonic output from the sample is compared with that of either KDP or urea. Thus the figure of merit of SHG of the sample is estimated.

The SHG efficiency of Li[ L-LMHCL] crystal was evaluated by taking the micro-crystalline powder and potassium di-phosphate (KDP) as the reference material. The SHG signal of grown sample is 3.9 mJ and 8.8 mJ for KDP respectively. Hence it is observed that the SHG efficiency of Li[ L-LMHCL] is nearly 0.55 times that of KDP. Since organic materials are moderate environmental stability, low mechanical strength, and limited temperature of operation. The semiorganic NLO crystal investigated in the present work provide better option and variety in the field of nonlinear optics.

### 3.6. Microhardness Studies

Microhardness measurements were made on TGBDD crystal using Shimadzu HMV- 2 microhardness tester fitted with a Vicker's diamond pyramidal indenter. The indentations were made for loads 25- 100g. Several trials were performed for the same load and the average diagonal length was taken for each load. The indentation time was 10 s. Vicker's microhardness values were calculated by the relation,

$$H_V = 1.8544 P/d^2 \text{ (Kg/mm}^2\text{)}$$

Where P is the applied load in kg and d is the mean diagonal length of the indenter impression. A graph was plotted between the hardness number  $H_V$  and the applied load P.

Figure.9 shows that the hardness number increases with the increase of the applied load. This behaviour of increasing microhardness with the load known as (RISE) reverse indentation size effect [23].

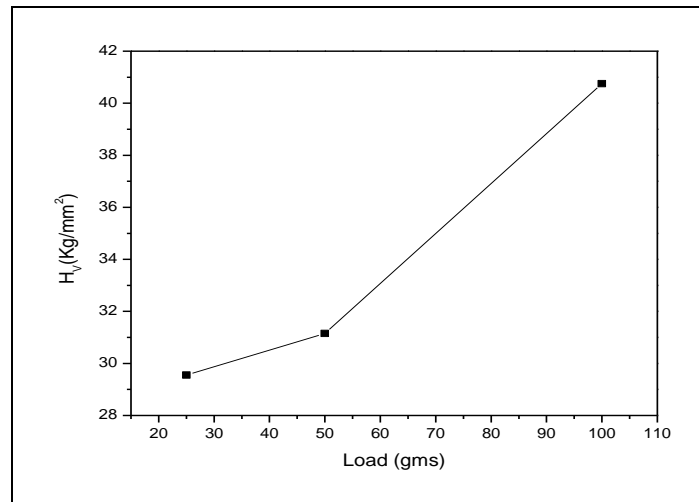


Figure 8: Load (p) Vs Hardness ( $H_V$ ) for Li[LMHCL] crystal.

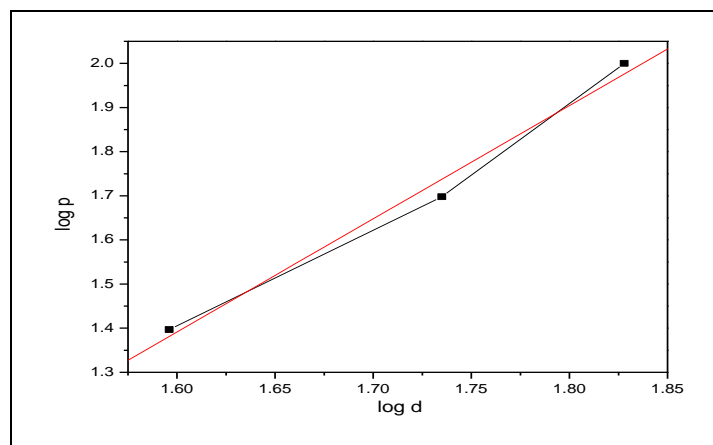


Figure 9: log d Vs log p for Li[LMHCL] crystal.

## 4. Conclusion

Good quality crystal of Li[LMHCL] was grown successfully by slow evaporation technique. The crystallinity was confirmed by x-ray diffraction analysis and it was observed that the crystal belongs to monoclinic crystal system. Due to effect of lithium in L-Lysine monohydrochloride crystal, the UV cut off wavelength is about 234 nm. The crystal has good transparent in the entire visible region. The optical bandgap ( $E_g$ ), absorption coefficient ( $\alpha$ ), extinction coefficient (K) was also calculated from UV spectrum. The powder SHG analyses reveal that the efficiency of this material is 0.55 times of that KDP. ). Vicker's microhardness test showed that the hardness value increases with increasing the applied load upto 100 g.

## 5. Reference

1. D. Kalaiselvi, R. Mohan Kumar, R. Jayavel, Mater. Res. Bull. 43 (2008) 1829–1835.
2. P.Rajesh,P. Ramasamy, C.K. Mahadevan, J. Cryst. Growth 311 (2009) 1156–1160.
3. D. Prem Anand, M. Gulam Mohamed, S.A. Rajasekar, S. Selvakumar, Joseph Arul Pragasam, P. Sagayaraj, Mater. Chem. Phys. 97 (2006) 501–505.
4. M. Narayan Bhat, S.M. Dharmaprakash, Growth of nonlinear optical L-lysine crystals, J. Cryst. Growth 236 (2002) 376–380.

5. Ledoux, J. Badan, J. Zyss, A. Migus, D. Hulin, J. Etchepare, G. Grillon, A. Antonetti, *J. Opt. Soc. Am. B4* (1987) 987–997.
6. S. Boomadevi, H.P. Mittal, R. Dhasekaran, *J. Cryst. Growth* 261 (2004) 55–62.
7. M.D. Aggarwal, J. Choi, W.S. Wang, K. Bhat, R.B. Lal, A.D. Shields, B.C. Penn, D.V. Frazier, *J. Cryst. Growth* 204 (1999) 179–182.
8. H.W. Zhang, A.K. Batra, R.B. Lal, *J. Crystal Growth* 137 (1994) 141.
9. C.C. Frazier, M.P. Cockerham, *J. opt.soc. Am* 134 (1987) 1899.
10. G.Xing, M.Jiang, Z.Shao, D.Xu, *Chin.J. Lasers* 14[1997] 302-308.
11. S.Velsko, Laser program annual report, Lawrence, Lawrence Livermore, National laboratory, Livermore CA, 1990.
12. S.R.Batten, R.Robson, *Angew, Chem.Int.Ed.* 37(1998) 1460-1494.
13. O.M.Yaghi, H.Li, C.Davis, D.Richaedson, T.L.Groy, *Acc. Chem.Res.* 31(1998) 474- 484.
14. S. Masilamani, P. Ilayabarathi, P. Maadeswaran, J. Chandrasekaran, K. Tamilarasan, *Optik* 123 (2012) 1304–1306.
15. Y. Lefur, M. Bagieu, Beucher, R. Masse, J.F. Nicoud, J.P. Le'vy, *Chem. Mater.* 8 (1995) 68.
16. S.B.Monaco, L.E.Davis, S.P.Velsko, F.T.Wang, D.Eimerl, A.J.Zalkin, *J.Cryst.Growth* 85 (1987) 252.
17. R. Ramesh Babu, K. Sethuraman, N. Vijayan, G. Bhagavannarayana, R.Gopalakrishnan, P. Ramasamy, *Cryst. Res. Technol.* 41 (2006) 906–910.
18. V. Krishnakumar, R. Nagalakshmi, S. Manohar, L. Kocsis, *Spectrochim. Acta A* 71 (2008) 471–479.
19. R. Ramesh Babu, K. Sethuraman, R. Gopalakrishnan, P. Ramasamy, *J. Cryst. Growth* 297 (2006) 356–360.
20. R. Robert, C. Justin Raj, S. Jerome Das, *Curr. Appl. Phys.* 10 (2010) 670–675.
21. V. Vasudevan, R. Ramesh Babu, G. Bhagavannarayana, K. Ramamurth, *Mater. Chem. Phys.* 124 (2010) 681–688.
22. Yiyang Zhou, H. William, Nelson, *Phys. Chem.* 79 (2010) 479–489.
23. Joshi V.N. (1990), 'Photoconductivity', Marcel Dekker, New York.
24. Balarew C. and Duhlew R. (1984), 'Application of the hard and soft acids and bases concept to explain Ligand coordination in Double salt structures', *J. Solid state Chemistry*, Vol. 55, pp. 1-6.